Structural Engineering and Mechanics, *Vol. 75, No. 2 (2020) 175-191*
DOI: https://doi.org/10.12989/sem.2020.75.2.175

Active structural control via metaheuristic algorithms considering soil-structure interaction

Serdar Ulusoy*[1], Gebrail Bekdaş[2] and Sinan Melih Nigdeli[2]

[1]*Department of Civil Engineering, Yeditepe University, 34755 Ataşehir, Istanbul, Turkey*
[2]*Department of Civil Engineering, Istanbul University, 34320 Avcılar,Istanbul, Turkey*

(Received March 8, 2019, Revised December 13, 2019, Accepted February 17, 2020)

Abstract. In this study, multi-story structures are actively controlled using metaheuristic algorithms. The soil conditions such as dense, normal and soft soil are considered under near-fault ground motions consisting of two types of impulsive motions called directivity effect (fault normal component) and the flint step (fault parallel component). In the active tendon-controlled structure, Proportional–Integral–Derivative (PID) type controller optimized by the proposed algorithms was used to achieve a control signal and to produce a corresponding control force. As the novelty of the study, the parameters of PID controller were determined by different metaheuristic algorithms to find the best one for seismic structures. These algorithms are flower pollination algorithm (FPA), teaching learning based optimization (TLBO) and Jaya Algorithm (JA). Furthermore, since the influence of time delay on the structural responses is an important issue for active control systems, it should be considered in the optimization process and time domain analyses. The proposed method was applied for a 15-story structural model and the feasible results were found by limiting the maximum control force for the near-fault records defined in FEMA P-695. Finally, it was determined that the active control using metaheuristic algorithms optimally reduced the structural responses and can be applied for the buildings with the soil-structure interaction (SSI).

Keywords: active tendon control; PID control; metaheuristic algorithms; soil-structure interaction; near-fault ground motions

1. Introduction

Using of smart systems in various structure types (Toklu and Arditi, 2014) is an increasing trend in the structural engineering. Various dynamic actions like earthquakes and winds form the vibrations in civil engineering structures, in which the usage of specific vibration isolator called ‘‘passive or active control’’ have become widespread due to stabilization of the building since long years. While active control systems are generally preferred because of utilization of ever-changing external mechanic energy source to protect the structure against destructive effects of the dynamic forces, passive control systems are also being used because these mechanisms are not complicated (Ghaffarzadeh and Younespour, 2014). The active tendon system, which is one of the active control method, was used in this study, needs the actuators to create the control force, the controller devices to calculate the control force, the sensors to measure either the acceleration, velocity or displacement in a structure and the cross prestressed steel cables bounded to actuators to continuously absorb the vibration of the structure (Nigdeli and Boduroglu, 2013). Actively, there are several control techniques to diminish the objective functions, that represent the structural response, including H_2, H_{inf}, linear quadratic regulator (LQR), neural network control, fuzzy logic control, sliding mode control (SMC) and PID control which was preferred in this study (Datta, 2003; Alavinasab and Muharrami, 2006). PID control usually seems appropriate for one or two degree of freedom systems to not occur confusion in its control algorithm (Nerves and Krishnan, 1995). However, this problem for tall buildings was overcame with the proposed optimization techniques and proportional PID parameters, which were obtained in the first floor and used for all stories to produce the same control force. Generally, the maximum drift of the structure are seen in the first story of the structure. For that reason, the displacement of the first story is taken as the objective function and the error signal in the active control.

Metaheuristic algorithms, that have been developed in order to overcome the difficulties due to the use of the traditional mathematical methods in solving complex problems, are inspired by events in nature, so the equations of these algorithms are the mathematical expression of the instinctive behaviors that exist in nature. Although all metaheuristic algorithms have their own inspirations, two important properties such as a random selection and a selection of the best result are existing in all algorithms. In terms of the success of the optimization, the balance between the random selection and the ability to select the best result should be established well to prevent the local optimum results (Yang, 2010). In this research, in which active tendons are controlled with PID, several metaheuristic algorithms are used such as FPA, TLBO and Jaya to effectively minimize the design variables in a short time.

*Corresponding author, Ph.D.
E-mail: Serulusoy87@gmail.com

ISSN: 1225-4568 (Print), 1598-6217 (Online)

The transferring of the seismic waves from a very soft ground type to an active-controlled structure can occur the deformations and rotations in the foundation of the structure during earthquakes. The neglection of these deformations and rotations in the foundation by assuming a fix based controlled building model may not reflect the exact structural responses. For this reason, it is necessary to consider the soil-structure interaction to observe the real behavior of the structures. In order to express this interaction between soil and structure, the parameters such as swaying stiffness, rocking stiffness, swaying damping and rocking damping were added to the building model.

Near fault ground motions were usually recorded at maximum 15 km away to the fault rupture and contain the impulsive features in time history records. They have more damaging effects to the structures than far fault ground motions because of demand of more ductility in structures. Also, the near fault ground motion caused two types of the impulsive motions called flint step and directivity effect which have the typical characteristics such as a permanent displacement, high peak ground acceleration and velocity (Chopra and Chintanapakdee, 2001). Therefore, the near fault ground motion (totally 56 ground motions including two components) sets as defined in FEMA P-695: Quantification of Building Seismic Performance Factors (FEMA P-695, 2009) were preferred to investigate the multi-story building model with active tendons considering SSI.

Several active structural control approaches are mentioned in this section. The active tendons and active mass dampers have been used as the active control methods to reduce peak acceleration due to strong winds in high building (Yang and Samali, 1983). More effective results in structural response were obtained with the active tendons in comparison with the active mass damper for the high buildings modelled as a cantilever beam (Abdel-Rohman and Leipholz, 1983). The performance of both control systems on the decline of the structural response is associated with the increase of the control force (Samali et. al., 1985). Also, the time delay in active control is a very important issue to consider the real behavior of the structures (Chung *et al*., 1988). Many studies are available in the literature either to prevent or improve the problems caused by the different control types in the active tendon-controlled structures. For example, the time delay effect was reduced using instantaneous optimal control algorithm with a modification (Chung et. al., 1989). Traditional algorithms may be weak in the nonlinear structures to actively control that is why the artificial neural networks are preferable to the active control of the nonlinear structures (Ghaboussi and Joghataie, 1995). The use of the genetic algorithm was appropriate to determine the parameters of controllers such as H_2, H_{inf} in the three-dimensional systems (Arfiadi and Hadi, 2000). A modified linear quadratic regulator (MLQR) instead of a traditional linear quadratic regulator (LQR) was used to grade the system stability order before the unknown earthquake excitation (Aldemir and Bakioglu, 2001). A fuzzy sliding-mode control algorithm was proposed to prevent the chattering effect in the traditional sliding-mode control algorithm (Alli and Yakut, 2005). The maximum structural reactions in the irregular structures were examined under near fault ground motions with PID controller identified its parameter using a numerical algorithm (Nigdeli and Boduroglu 2013). In some research, two different control algorithms were either compared to observe the superiority or combined to successfully decrease the structural responses. Proposed sliding mode controller without chattering problem represented better output in the structural reactions than PID controller (Guclu 2006). The comparison of the reduction of the top floor displacement responses of the both block pulse functions and linear quadratic regulator was done (Ghaffarzadeh and Younespour 2014). A new approach named a wavelet-based adaptive pole assignment for the structural control found more successful than LQR about minimizing of the time delay effect and increasing building resistance (Amini and Samani 2014). Neuro-genetic algorithm, that formed the combination of dynamic fuzzy wavelet neuroemulator and the floating point genetic algorithm, was developed to significantly decrease the responses of three-dimensional active controlled structures with inclusion of geometrical and material non-linearities (Adeli and Jiang 2008). Incorporation of the sliding-mode control and artificial neural network called neural based sliding-mode control was offered to consider the parametric uncertainties and time delay effects using genetic algorithm in the optimization process (Yakut and Alli 2011).

By considering SSI, several structural control applications were proposed (Cacciola *et. al*. 2015, Zou *et al*. 2012, Bekdaş G. *et al*. 2019). The irregular structure with the active tendons was investigated by the aid of H_{inf} direct output feedback control algorithm under earthquake excitations to emphasize the SSI effects on structural responses (Chang *et al*. 2010).The irregular active tendon-controlled structure, which is located on the different soil types, was examined benefiting from LQR algorithm.(Nazarimofrad and Zahrai 2016).

As seen, a lot of studies have been done in relation to the active tendons control in the engineering structures, but only a few of these studies involve the soil-structure interaction. The aim of this study is to expand the field of the multi degree of freedom systems with active tendons including soil-structure interaction under the near fault ground motions. In this study, the parameters of the PID controllers are determined by using novel optimization approaches employing metaheuristic algorithms such as FPA, TLBO and JA.

2. The employed metaheuristic algorithms

This chapter includes the working principles and mathematical expressions of the metaheuristic algorithms such as FPA, JA and TLBO, which were used to determine the PID controller parameters in the time domain analysis. The general flow diagram of these algorithms is given in Fig. 1.

The design variables, the design constants which are the properties of structure and soil properties presented in Section 3.3 and the algorithm parameters such as population

number, maximum number of iterations and specific parameters for the metaheuristic algorithms should be defined in the optimization process. FPA has specific parameters in the proposed methods of the study. The design variables of the active controller parameters are given in Section 3.1.

After the definition of constant value, the design variables of the problem are randomly assigned with numerical values with a range. This range is used to shorten the optimization process time. By assignment of the random values, an initial solution matrix containing set of the design variables is constructed and the number of sets is equal to the population number. All sets of the design variables are solved to find the objective function which is the maximum displacement of the first story of the structure. Generally, the maximum drift is seen at the first story and the numerical example is an isolated first story. During the calculation of the objective function, a control force limit is considered and the violated results assigned with a penalty value which is physically a big value.

After the generation of the initial solutions, the role of the metaheuristic algorithm starts. The existing results are updated according to the algorithm rules given in Section 2.1, 2.2 and 2.3. The objective function values of the old and new design variables are compared. Thus, the results are updated if the new one has a smaller objective function. The updating process continues for the maximum number of the iteration defined as the stopping criterion.

2.1 Flower pollination algorithm

Flower pollination algorithm, whose mathematical expression is based on the pollination of flowering plants, has been found by Yang (Yang and Karamanoglu, 2014). In this algorithm, the types of the pollinations and steady repetition of visit to the same flower of the pollinator play an important role in the global and local optimization processes. The pollination occurs in two ways: self-pollination (among different flowers of the same plant) and cross-pollination (among the different plant flowers by pollinators). In the global optimization, the pollination type is carried out by cross pollination via bee, insect and other animals, while in the local optimization, self-pollination occurs with the aid of the wind and diffusion. The most important advantage of the steady repetition of visit to the same flower of the pollinator in the global and local optimization is that the pollen is put in the most accurate flower. Also, in the global pollination process, Levy flights should be taken into account and a switch probability should be determined in order to tolerate its relationship with the local pollination. Mathematical expressions of the global pollination and local pollination are given in Eqs.1 and 2, respectively.

$$x_i^{t+1} = x_i^t + L(x_i^t - g^*) \quad (1)$$

$$x_i^{t+1} = x_i^t + \varepsilon(x_j^t - x_k^t) \quad (2)$$

L is Levy distribution, g^* is the best existing solution, x_i^t is the existing solution for i^{th} iteration and x_i^{t+1} is the newly generated i^{th} solution for $(t+1)^{th}$ iteration. x_j^t and x_k^t are two existing solution of two randomly chosen solutions (j and k). A switch probability is used as an algorithm specific parameter to choose the pollination type in each iteration.

2.2 Teaching learning based optimization

Teaching learning-based optimization developed by Rao (Rao et. Al., 2011) and consists of the teaching and learning phase. In a classroom, where all of the representatives are students, the most knowledgeable student is appointed as a teacher and the knowledge of this teacher is transferred to the other students. The mathematical expression of teaching phase is presented as Eq. 3. A random number between 0 and 1 is shown as rand (1).

$$x_i^{t+1} = x_i^t + rand(1)(g^* - TFx_{ave}) \quad (3)$$

In the learning phase, two of the students will be assigned to express their knowledge to the class after increasing the level of knowledge of the students in the teaching phase. Thus, the best solution will update itself at every step. The mathematical expression of the learning phase is given in Eq. 4.

$$x_i^{t+1} = \begin{Bmatrix} x_i^t + rand(1)\left(x_j^t - x_k^t\right) \ if \ f\left(x_j^t\right) < f(x_k^t) \\ x_i^t + rand(1)\left(x_k^t - x_j^t\right) \ if \ f(x_k^t) < f(x_j^t) \end{Bmatrix} \quad (4)$$

g^* is the best solution defined as a teacher, TF is teaching factor which is randomly generated number and can be 1 or 2, x_{ave} is the average of all solutions and x_j^t and x_k^t are the existing solution of two randomly chosen solutions. The two phases of TLBO are consequently applied in iteration. In that case, it is not necessary to use a specific parameter to choose a phase.

2.3 Jaya algorithm

Jaya algorithm was evolved by Rao (Rao 2016) simplifying the teaching learning based optimization and utilizing only a single phase. The purpose of this algorithm given in Eq. 5 is blending the best solution with the worst solution to escape from the worst solution and to come close to the best solution. Here, g^w is the worst solution, r_1 and r_2 represent the random variable number between 0 and 1. JA is a single-phase algorithm and has no specific parameter.

$$x_i^{t+1} = x_i^t + r_1(g^* - x_i^t) - r_2(g^w - x_i^t) \quad (5)$$

3. The proposed methodology

This section focusses on four topics. Firstly, the definition, parameters and equation of the PID controller are described. Secondly, the simplified vibration equations of the near-fault ground motions are shown and the near fault ground motions with or without pulses are presented with tables. After that, the equation of motions of the active tendon-controlled structure considering soil-structure interaction is written. Finally, the optimization process used in the numerical structure case is explained.

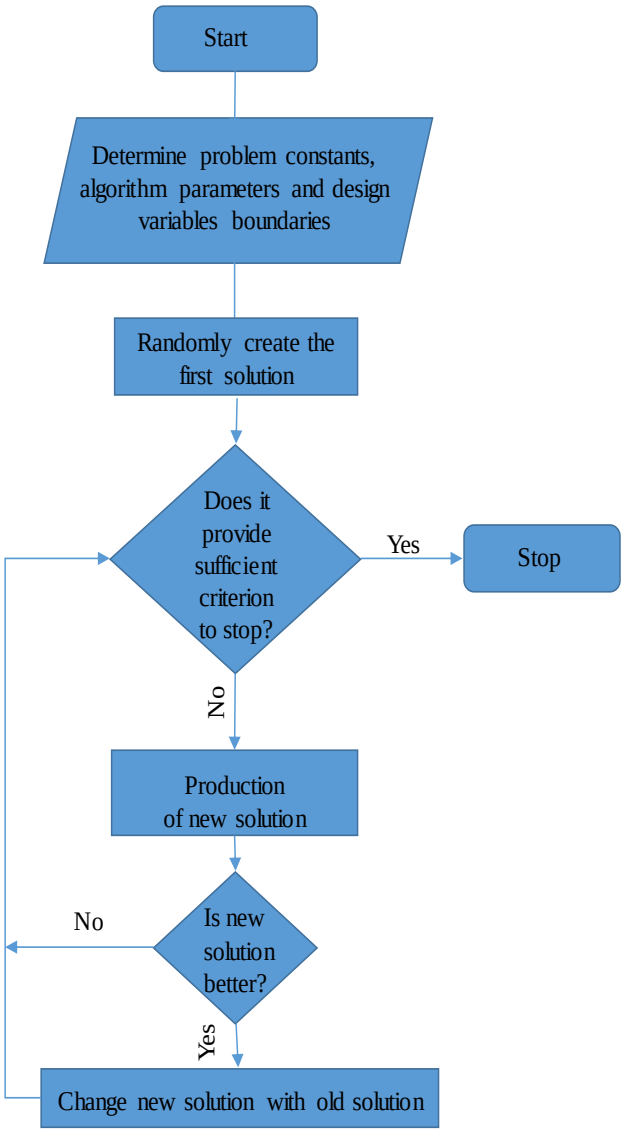

Fig. 1 The general flow diagram of FPA, JA and TLBO

3.1 Proportional integral derivative (PID) controllers

The PID controller compares the response signal of the structure with the reference signal and generates an error signal from the difference it finds. It creates the control signal that is the displacement of the activator and will affect the structure to minimize the error signal and to reduce the structural responses. Thus, the error is minimized. PID controller is designed with the controller equation given as Eq. 6.

$$u(t) = K_p \left[e(t) + \frac{1}{T_i} \int_0^t e(t)dt + T_d \frac{de(t)}{dt} \right] \quad (6)$$

K_p is the proportional gain, T_d is the derivative gain, T_i is the integral gain, e(t) is the error signal and u(t) is the control signal.

3.2 Near-fault ground motions

The vibration equations developed by Makris (Makris, 1997) were used in order to be able to express the near fault ground motion. These equations in time (t) domain are given with Eqs. 7 and 8 for the ground acceleration ($a_g(t)$) of the directivity effect and the flint step, respectively as seen in Fig. 2.

$$a_g(t) = \omega_p V_p \cos(\omega_p t) \qquad 0 \le t \le T_p \quad (7)$$

$$a_g(t) = \omega_p \frac{V_p}{2} \sin(\omega_p t) \qquad 0 \le t \le T_p \quad (8)$$

The Calculation of the pulse period (T_p) and pulse frequency (ω_p) of the near fault ground motions for the soil and rock sites according to moment magnitude (Mw) was emerged by Sommerville (Sommerville, 2003). These equations are given as Eqs. 9 and 10. Cox derived the Eq. 11 to calculate the peak ground velocity (V_p) depend on the moment magnitude and directivity angle (ϕ) (Cox and Ashford, 2002). Also, the several sets of the ground motions are presented in FEMA P-695: Quantification of Building Seismic Performance Factors. The near fault ground motions without pulse and with pulse are given in Tables 1 and 2, respectively.

$$LogT_p = -2.02 + 0.346M_w \qquad For\ soft\ site \qquad (9)$$

$$LogT_p = -3.17 + 0.5M_w \qquad For\ rock\ site \qquad (10)$$

$$LogV_p = 6.444 - 0.0187\phi - 5.022Log(M_w) \qquad (11)$$

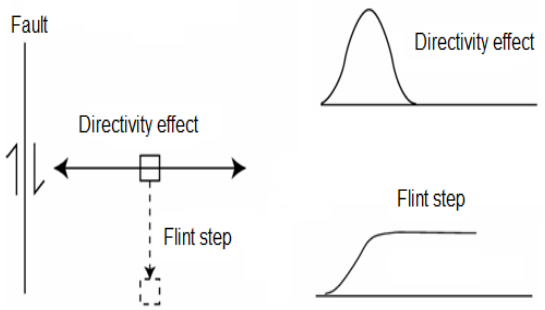

Fig. 2 Impulsive motions of near-fault ground motions

Table 1The near fault ground motions without pulse

No	Earthquake Name	Recording Station	Year	Magnitude
1	Northridge-01	LA - Sepulveda VA	1994	6.7
2	Loma Prieta	Bran	1989	6.9
3	Loma Prieta	Corralitos	1989	6.9
4	Cape Mendocino	Cape Mendocino	1992	7.0
5	Gazli, USSR	Karakyr	1976	6.8
6	Imperial Valley-06	Bonds Corner	1979	6.5
7	Imperial Valley-06	Chıhuahua	1979	6.5
8	Denali, Alaska	TAPS Pump Sta. #10	2002	7.9
9	Nahanni, Canada	Site 1	1985	6.8
10	Nahanni, Canada	Site 2	1985	6.8
11	Northridge-01	Northridge – Saticoy	1994	6.7
12	Chi-Chi, Taiwan	TCU067	1999	7.6
13	Chi-Chi, Taiwan	TCU084	1999	7.6
14	Kocaeli, Turkey	Yarimca	1999	7.5

Table 2 The near fault ground motions with pulse

No	Earthquake Name	Recording Station	Year	Magnitude
1	Irpinia, Italy-01	Sturno	1980	6.9
2	Superstition Hills-02	Parachute Test Site	1987	6.5
3	Duzce, Turkey	Duzce	1999	7.1
4	Erzican, Turkey	Erzican	1992	6.7
5	Imperial Valley-06	El Centro Array #6	1979	6.5
6	Imperial Valley-06	El Centro Array #7	1979	6.5
7	Kocaeli, Turkey	Izmit	1999	7.5
8	Landers	Lucerne	1992	7.3
9	Cape Mendocino	Petrolia	1992	7.0
10	Northridge-01	01 Rinaldi Receiving Sta	1994	6.7
11	Loma Prieta	Saratoga – Aloha	1989	6.9
12	Northridge-01	01 Sylmar - Olive View	1994	6.7
13	Chi-Chi, Taiwan	TCU065	1999	7.6
14	Chi-Chi, Taiwan	TCU102	1999	7.6

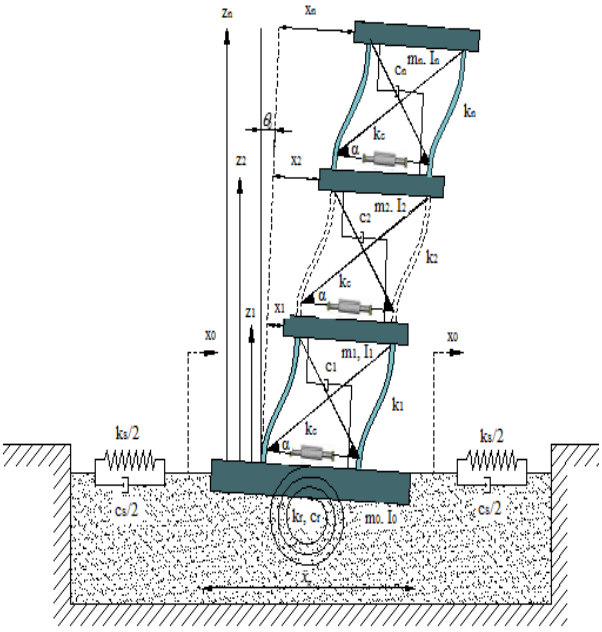

Fig. 3 Shear building model with the active tendons considering SSI effect

3.3 The time domain analyses of structures with active tendons

A N-story shear building model with active tendon considering SSI effect is shown in Fig. 3, where the ground acceleration $\ddot{x}_g$, the swaying (c_s) and rocking damping (c_r), swaying (k_s) and rocking stiffness (k_r), the mass (m_0) and the mass moment of inertia (I_0) of the foundation, the displacement (x_0) and rotation (θ_0) of the base, the angle of tendon (α), tendon stiffness (k_c), the story stiffness k(i), story damping c(i),the story mass m(i) and story mass moment of inertia I(i), the displacement x(i) and the distance between the stories and base z(i) of i^{th} story are given.

The equation of motion of the active tendon-controlled structure is written as Eq. 12. The acceleration, velocity and displacement vectors are shown as a(t), v(t) and x(t). [M_{soil}], [C_{soil}], [K_{soil}], [M^*_{soil}] and [b] represent the mass, damping, stiffness, acceleration mass and influence matrices of the structure with SSI from Eq. 13 to Eq. 17, respectively. These matrices contain a part of the sub-matrices such as [M_v], [M_z], Mass [M], damping [C] and stiffness [K] of fixed based structure from Eq. 18 to Eq. 22.

$$\begin{aligned}[M_{soil}]a(t) + [C_{soil}]v(t) + [K_{soil}]x(t) \\ = -[M^*_{soil}]\ddot{x}_g(t) \\ -(4k_c cos\alpha)[b]u(t)\end{aligned} \qquad (12)$$

$$[M_{soil}] = \begin{bmatrix} [M] & [M_v] & [M_z] \\ [M_v]^T & m_0 + \left(\sum_{i=1}^{n} m_i\right) & \left(\sum_{i=1}^{n} m_i z_i\right) \\ [M_z]^T & \left(\sum_{i=1}^{n} m_i z_i\right) & \left(\sum_{i=1}^{n} m_i z_i^2 + I_0 + \sum_{i}^{n} I_i\right) \end{bmatrix} \qquad (13)$$

$$[C_{soil}]=\begin{bmatrix}[C] & 0 & 0\\ 0 & c_s & 0\\ 0 & 0 & c_r\end{bmatrix} \quad (14)$$

$$[K_{soil}]=\begin{bmatrix}[K] & 0 & 0\\ 0 & k_s & 0\\ 0 & 0 & k_r\end{bmatrix} \quad (15)$$

$$[M^*_{soil}]=\begin{bmatrix} m_1\\ m_2\\ m_3\\ .\\ .\\ m_n\\ m_0+\left(\sum_{i=1}^{n} m_i\right)\\ \left(\sum_{i=1}^{n} m_i z_i\right)\end{bmatrix} \quad (16)$$

$$[b]=[1\ldots\ 1\ -N\ 0]^T \quad (1X(N+2)) \quad (17)$$

$$[M_v]=\begin{bmatrix} m_1\\ m_2\\ m_3\\ .\\ .\\ m_n\end{bmatrix} \quad (18)$$

$$[M_z]=\begin{bmatrix} m_1 z_1\\ m_2 z_2\\ m_3 z_3\\ .\\ .\\ m_n z_n\end{bmatrix} \quad (19)$$

$$[M]=\begin{bmatrix} m_1 & & & & & & \\ & m_2 & & & & & \\ & & . & & & & \\ & & & . & & & \\ & & & & . & & \\ & & & & & . & \\ & & & & & & m_n\end{bmatrix} \quad (20)$$

$$[C]=\begin{bmatrix} c_1+c_2 & -c_2 & & & & & \\ -c_2 & c_2+c_3 & -c_3 & & & & \\ & -c_3 & c_3+c_4 & -c_4 & & & \\ & & -c_4 & . & . & & \\ & & & . & . & . & \\ & & & & . & . & -c_n\\ & & & & & -c_n & c_n\end{bmatrix} \quad (21)$$

$$[K]=\begin{bmatrix} k_1+k_2 & -k_2 & & & & & \\ -k_2 & k_2+k_3 & -k_3 & & & & \\ & -k_3 & k_3+k_4 & -k_4 & & & \\ & & -k_4 & . & . & & \\ & & & . & . & . & \\ & & & & . & . & -k_n\\ & & & & & -k_n & k_n\end{bmatrix} \quad (22)$$

3.4 The optimization process

While optimizing the parameters of the PID controller, the optimization codes of three different algorithms were written in Matlab with Simulink (MathWorks Inc., 2015). Also, the numerical solution of the differential equations was realized by using Runge-Kutta Method with the step size h = 0.001. The block diagram of the structure generated in Simulink for the dynamic analyses is shown in Figure 4. As the performance index of the control, the displacement of the 1st floor is taken and the reference value is assigned with 0 for the control system where the displacement is feedbacked. The sum of the error signal itself, division of the integral gain by integral of the error signal and multiplication of the derivative gain by derivative of the error signal are multiplied by the proportional gain and this value is equal to the control signal which multiplied by $4k_c\cos\alpha$ after considering 20 ms time delay effect (Nigdeli and Boduroglu, 2013) with a transport delay block. All values were collected as indicated by the equation of motion and divided by the mass matrix. Thus, all the reactions of the structures, control force and control signal were calculated.

The optimum parameters of the PID controller of the active tendon-controlled structure were determined under directivity effect with the pulse period T_p = 3.0 s and the peak ground velocity V_p = 230 cm /s which are the average values obtained by using the Eqs. 8-10. In addition, the control force was limited to 10 percent of the average weight of one floor during the simulation time that was taken as 20 s and was repeated for 15000 iterations in all metaheuristic algorithms. During the optimization, when the maximum displacement of the 1st floor is more than the uncontrolled system, the current iteration is stopped to prevent a result with stability error and the optimization process is continued with the next iteration.

4. Numerical examples

The story mass coefficients, story stiffness coefficients, story damping coefficients, story height, story moment of inertia, foundation mass and foundation moment of inertia of fifteen story shear building are given in Table 3 (Guclu and Yazıcı, 2008; Farshidianfar and Soheili, 2013). The stiffness and angle of tendons are taken from the studies of Chung to actively control this structure (Chung et. al., 1988)

Table 3 The story parameters of 15-story structure [31,32]

Story	m_i (t)	k_i (N/m)	c_i (Ns/m)	I_i (kgm^2)	z_i (m)
Base	650	See Table 4		2.20x10^7	0
1	450	18050000	26170	1.46x10^7	3.50
2	345	340400000	293700	1.46x10^7	7.00
3	345	340400000	293700	1.46x10^7	10.5
4	345	340400000	293700	1.46x10^7	14.0
5	345	340400000	293700	1.46x10^7	17.5
6	345	340400000	293700	1.46x10^7	21.0
7	345	340400000	293700	1.46x10^7	24.5
8	345	340400000	293700	1.46x10^7	28.0
9	345	340400000	293700	1.46x10^7	31.5
10	345	340400000	293700	1.46x10^7	35.0
11	345	340400000	293700	1.46x10^7	38.5
12	345	340400000	293700	1.46x10^7	42.0
13	345	340400000	293700	1.46x10^7	45.5
14	345	340400000	293700	1.46x10^7	49.0
15	345	340400000	293700	1.46x10^7	52.5

Table 4 Properties of soil types

Soil type	c_s (Ns/m)	c_r (Ns/m)	k_s (N/m)	k_r (N/m)
Soft soil	2.19x10^8	2.26x10^{10}	1.91x10^9	7.53x10^{11}
Medium soil	6.90x10^8	7.02x10^{10}	1.80x10^{10}	7.02x10^{12}
Dense soil	1.32x10^9	1.15x10^{11}	5.75x10^{10}	1.91x10^{13}

Table 5 Optimum parameters of PID controller and the maximum first story displacement under directivity pulse

Soil	Algorithm	K_p	T_d	T_i	X_1 (cm)
Dense	FPA	-2.1750	0.0759	0.0150	2.1531
	JA	-1.8340	0.0972	0.0112	2.1543
	TLBO	-1.8404	0.0978	0.0109	2.1543
Medium	FPA	0.0058	-12.741	2.0401	2.1504
	JA	0.0059	-12.439	2.1697	2.1505
	TLBO	0.0051	-14.813	-2.9982	2.1515
Soft	FPA	-0.0080	9.7314	7.7082	2.1081
	JA	-0.0075	9.8538	-0.8091	2.1069
	TLBO	0.0082	-9.9218	-0.6430	2.1060

and are accepted as 360 and 372100 N/m, respectively. The properties of the three soil types such as dense, medium and soil are shown in Table 4 to consider soil structure interaction (Liu et. al., 2008). The first story of the structure has a small stiffness value and it is a base isolation floor.

The parameters of the PID controller in fifteen story structure considering soil-structure interaction was optimized with three different algorithms under the earthquake record specified in Section 3.4. The parameters of PID controller and the maximum first story displacements under directivity pulse were found to be close values for each algorithm according to the results of the three algorithms and shown in Table 5. The Optimization methodology can find different combinations of optimum control parameters which have similar effects on the control of structure. These parameters are used to determine the structure reactions of the different earthquake records, which are given in Table 1 and 2. However, the simulation time was taken as 120 seconds in order to prevent any stability problems in the structure under these records. The block diagrams of the uncontrolled and controlled structure considering SSI in Simulink are presented Fig. 5 and 6.

The maximum responses of the structure under near fault ground motions with and without pulse according to the best of three algorithms are given from Tables 6 to 11 in Appendix. Flower pollination algorithm has better results for the first-floor displacement of the structure that positioned on the dense and medium type of the soils, while TLBO is more effective for the soft type of soils. JA based method is not the best one since it is a single-phase algorithm. The max displacements of the top story of an uncontrolled structure with dense, medium and soft soil has been found 227.11, 226.60 and 215.95 cm under near fault records without pulse and were dropped to 120.32, 120.05, and 120.84 using the active tendon, respectively. However, a decrease in the acceleration values under these records is not noticeable. The time history plots of the top story displacement and acceleration of the both controlled and uncontrolled structure according to the soil type are presented in Fig. 7 and 8 for the critical excitation.

Besides, the max control signal and force for the controlled structure with dense, medium and soft soil were calculated 19.49, 19.20 and 18.13 cm and 234.65, 231.14, and 218.26 KN, respectively.

On the other sites, the max displacement of the top story of a controlled structure with dense, medium and soft soil are presented in Fig. 9 reduced by 156.21, 157.65 and 155.23 cm under near fault records with pulse. This time, the reduction of acceleration value is appreciable and the top story acceleration is shown in Fig. 10 and reduces about 45 percent.

5. Conclusions

In this study, the active structural control methods using metaheuristic algorithms are proposed. The conclusions about control of a fifteen-story structure with optimized PID are as follows:

• Confusion in control algorithm of PID for multi degree of freedom systems was overcame with recommended optimization techniques and usage of the proportional PID parameter of the first floor in different floors to obtain the same resulting control force in each story.

• Three different metaheuristic algorithms were used to verify the optimum results. The fact that the controller parameters are close to each other indicates that the optimization is done correctly. In that case, the optimum results of the examples are verified by using three different algorithms.

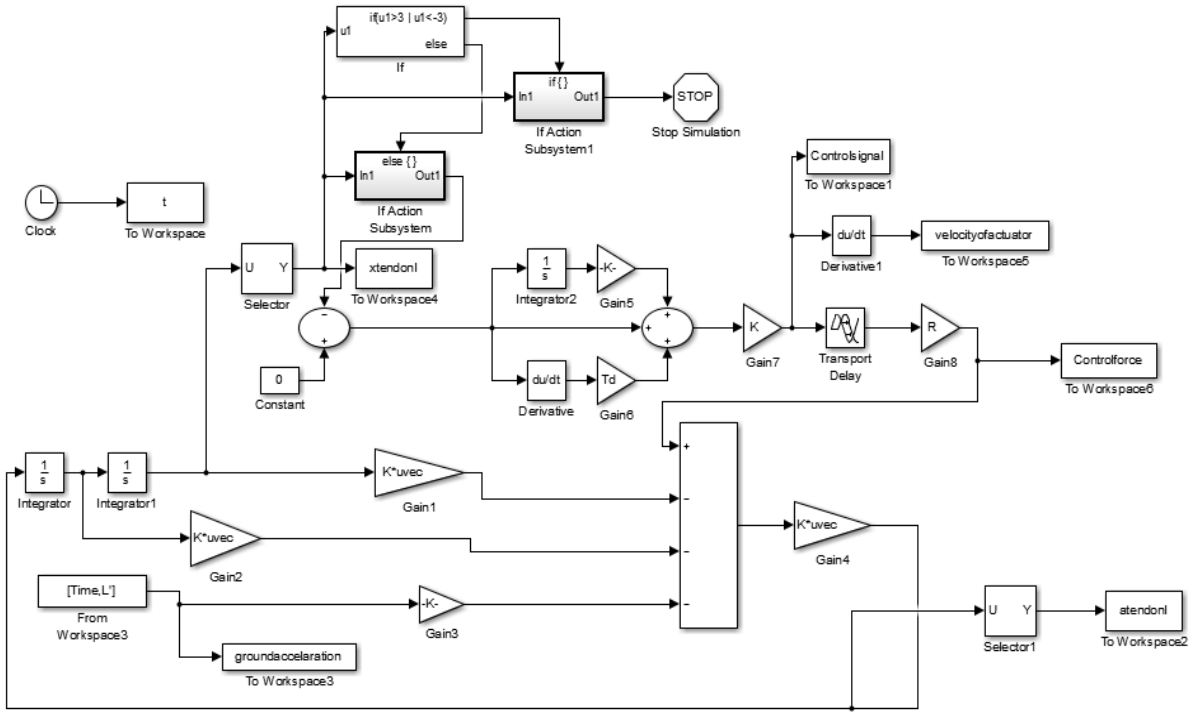

Fig. 4 The block diagram of the active tendon-controlled structure in the process of optimization

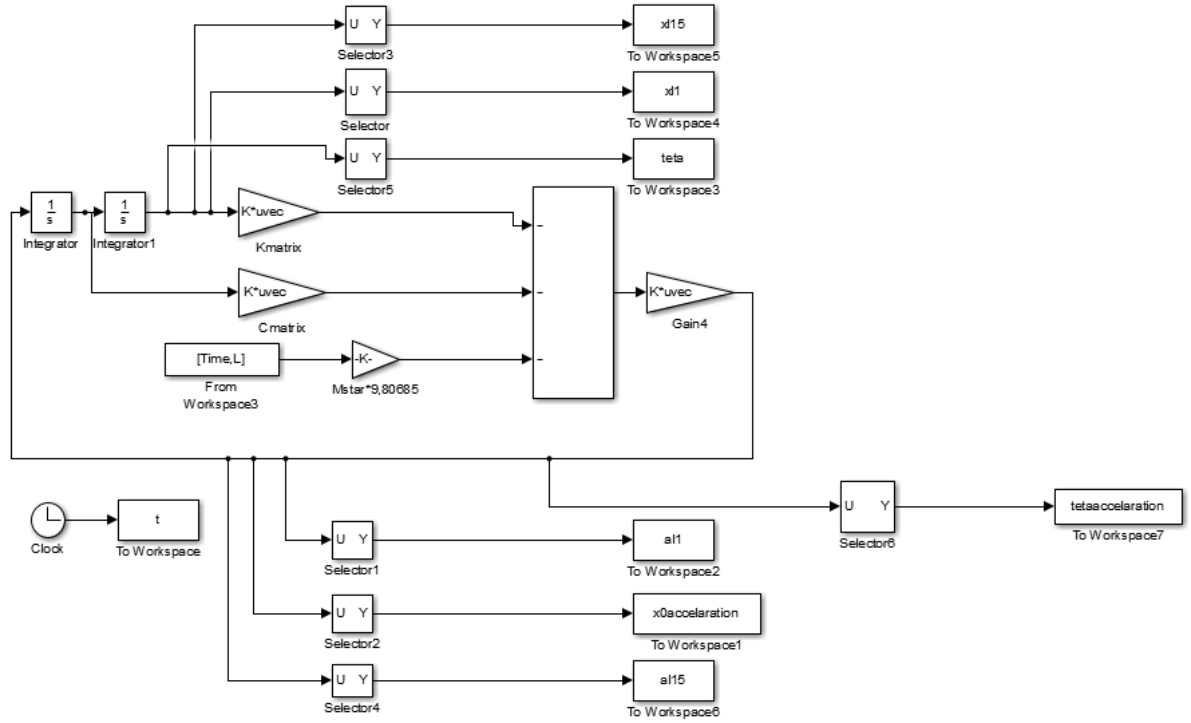

Fig. 5 The block diagram of the uncontrolled structure

• It was indicated that the structural responses of active controlled structure with different soil type such as dense, medium and soft were significantly reduced under near fault records.

• It seems that the uncontrolled structure which has the lower rigidity in the first floor compared to the other floor has extremely big displacement at the first story. This displacement is reduced up to 45% for the critical excitation using the active control system. It has been determined that the control with active tendons has been also achieved in the structure which has big responses such as the base isolated structures.

• The performance index and the feedback of the PID controller are the first story displacement. In addition to that, all story responses and acceleration values are reduced with the optimized control methodology.

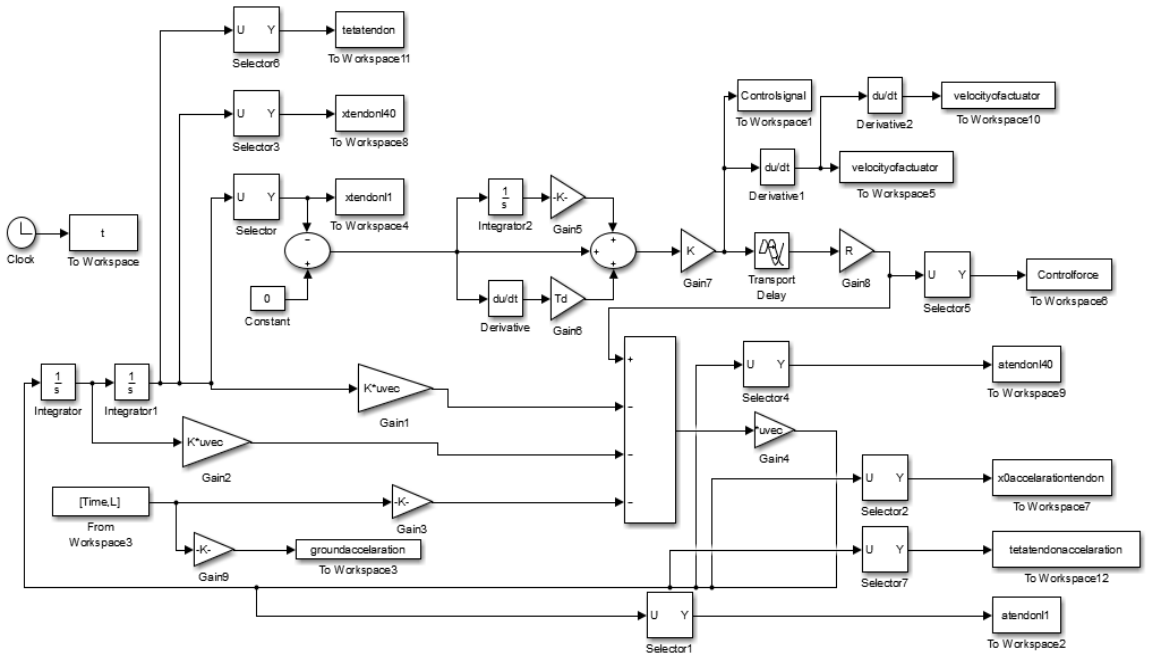

Fig. 6 The block diagram of the active tendon-controlled structure.

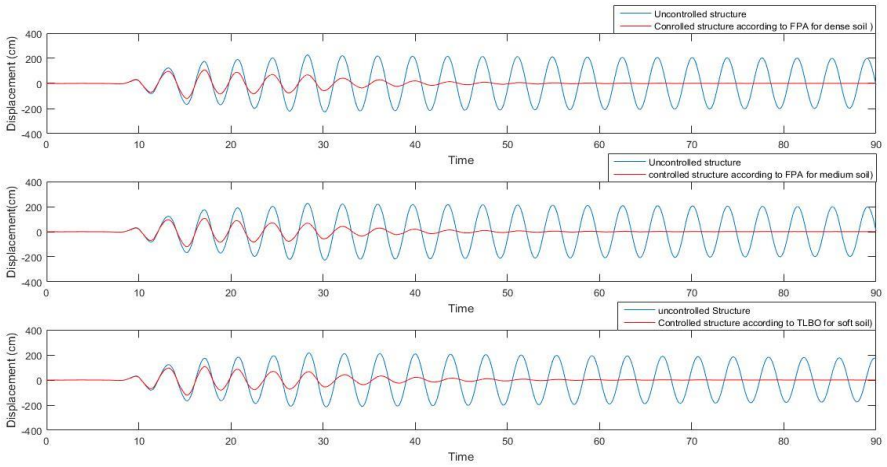

Fig. 7 Time history of top displacement of both controlled and uncontrolled structure under Kocaeli Turkey, Yarımca - FN component according to different soil type.

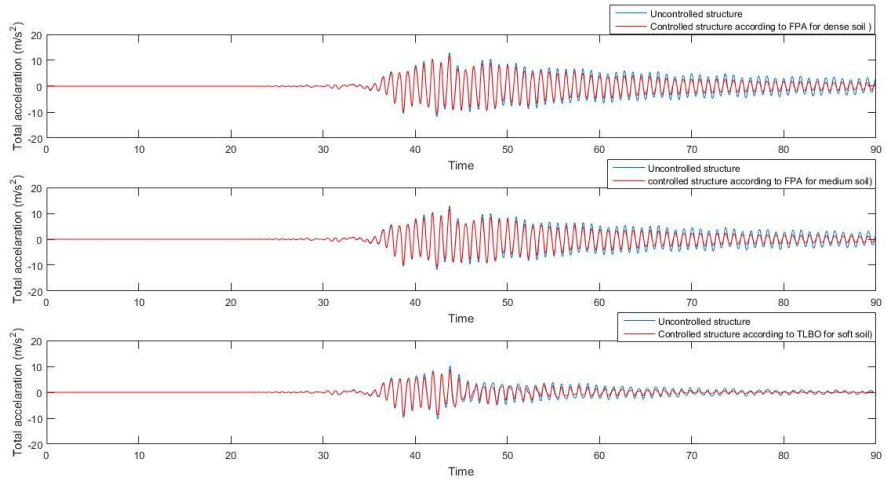

Fig. 8 Time history of top total acceleration of both controlled and uncontrolled structure under Chi-Chi, Taiwan TCU084 - FN component according to different soil type.

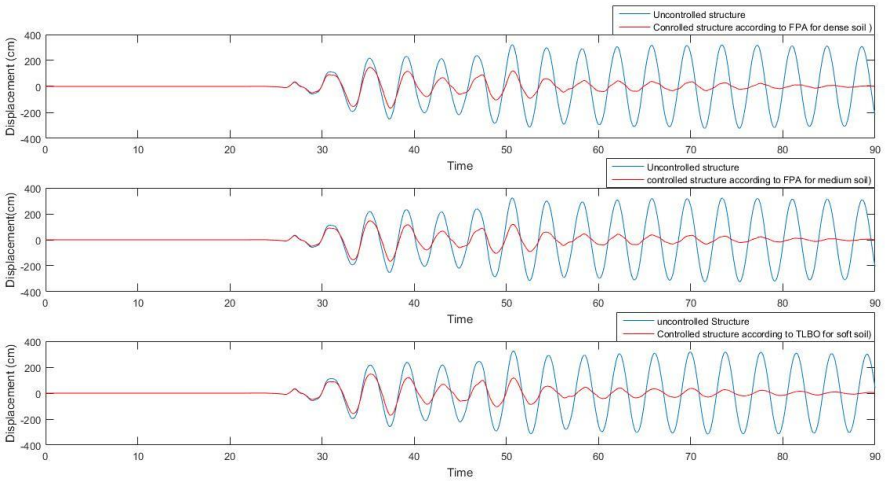

Fig.9 Time history of top displacement of both controlled and uncontrolled structure under Chi-Chi, Taiwan TCU065 – FN component according to different soil type.

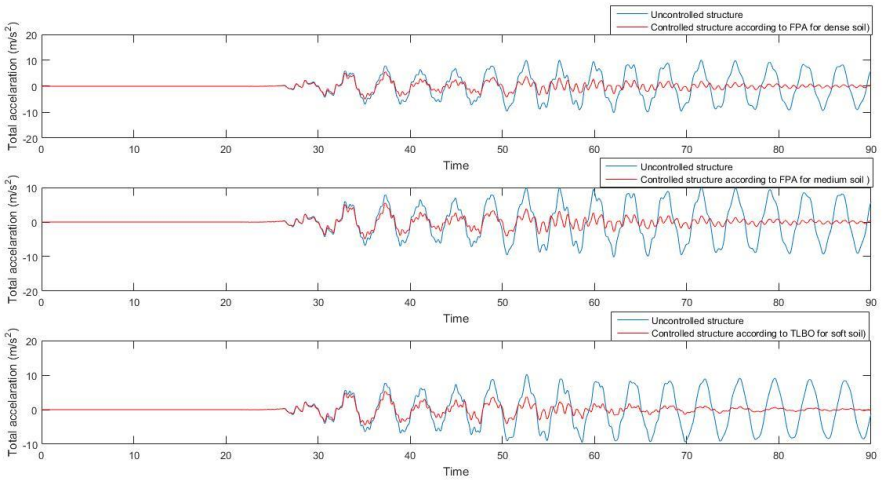

Fig.10 Time history of top total acceleration of both controlled and uncontrolled structure under Chi-Chi, Taiwan TCU065 – FN component according to different soil type.

The proposed methodology considers the time delay and control force limitation values to obtain a feasible approach and the control force limitation can be easily and automatically handled without providing a suitable range for the controller parameters. As the final remark of the work, metaheuristic algorithms commonly used in the optimization of the structures and parameter tuning of the passive structural control systems are also a suitable tuning approach for the determination of the PID controller parameter used in the seismic structures in near-fault regions and the effective results can be also found by considering soil-structure interaction. In future, three-dimensional structures can be also handled with proposed methodology and the computational time of the optimization methodology can be shortened by using artificial intelligence methods.

References

Abdel-Rohman, M. and Leipholz, H.H. (1983), "Active control of tall buildings", *J. Struct. Eng. ASCE*, **109**, 628-645. https://doi.org/10.4203/csets.33.9

Adeli, H. and Jiang, X. (2008), "Neuro-Genetic algorithm for non-linear active control of structures", *J. Numeric Methods Eng*., **75**, 770-786. https://doi.org/10.1002/nme.2274.

Alavinasab, A. and Muharrami, H. (2006), "Active Control of Structures Using Energy-Based LQR Method", *Comput. Aid Civil Infrastruct. Eng.*, **21**, 605-611. https://doi.org/10.1111/j.1467-8667.2006.00460.x.

Aldemir, U. and Bakioglu, M. (2001), "A new Numerical Algorithm for Sub-optimal Control of Earthquake Excited Linear Structures", *J. Numeric. Methods Eng.*, **50**, 2601-2616. https://doi.org/10.1002/nme.137.

Alli, H. and Yakut, O. (2005), "Fuzzy sliding-mode control of structures, engineering structures", **27**, 277-284. https://doi.org/10.1016/j.engstruct.2004.10.007.

Amini, F. and Samani, M.S. (2014), "A Wavelet-Based Adaptive Pole Assignment Method for Structural Control", *Comput. Aid Civil Infrastruct. Eng.*, **29**, 464-477. https://doi.org/10.1111/mice.12072.

Arfiadi, Y. and Hadi, M.N.S. (2000), "Passive and Active Control of Three- dimensional Buildings", *Earthq. Eng. Struct. Dynam.*, **29**, 377-396. https://doi.org/10.1002/(sici)1096-9845(200003)29:3<377::aid-eqe911>3.0.co;2-c

Bekdaş, G., Kayabekir, A.E., Nigdeli, S.M. and Toklu, Y.C.

(2019), "Tranfer function amplitude minimization for structures with tuned mass dampers considering soil-structure interaction", *Soil Dynam. Earthq. Eng.*, **116**, 552-562. https://doi.org/10.1016/j.soildyn.2018.10.035

Cacciola, P., Espinosa, M.G. and Tombari, A. (2015), "Vibration control of piled-structures through structure-soil-structure-interaction", *Soil Dynam. Earthq. Eng.*, **77**, 47-57. https://doi.org/10.1016/j.soildyn.2015.04.006

Chang, C.C., Lin C.C. and Wang, J.F., (2010), "Active control of irregular buildings considering soil-structure interaction effects", *Soil Dynam. Earthq. Eng.*, **30**, 98-109. https://doi.org/10.1016/j.soildyn.2009.09.005

Chopra, A.K. and Chintanapakdee, C. (2001), "Comparing response of SDF systems to near-fault and far-fault earthquake motions in the context of spectral regions", *Earthq. Eng. Struct. Dynam*., **30**. https://doi.org/10.1002/eqe.92

Chung, L.L., Lin R.C., Reinhorn, A.M. and Soong, T.T. (1989), "Experimental Study of Active Control for MDOF Seismic Structures", *J. Struct. Eng. ASCE*, **115**, 1609-1627.https://doi.org/10.1061/(asce)0733-9399(1989)115:8(1609)

Chung, L.L., Reinhorn, A.M. and Soong, T.T. (1988), "Experiments on active control of seismic structures", *J. Eng. Mech.*, **114**(2), 241-256. https://doi.org/10.1061/(asce)0733-9399(1988)114:2(241).

Cox, K.E. and Ashford, S.A., (2002), "Characterization of Large Velocity Pulses for Laboratory Testing. Report 2002/22", *Pacific Earthquake Engineering Research Center*, University of California, Berkeley, California, USA.

Datta, T.K., (2003), "A State-of-the-Art Review on Active Control of Structures", *ISET J. Earthq. Technol.*, Paper No. 430, **40**(1).

Farshidianfar, A. and Soheili, S., (2013), "ABC optimization of TMD parameters for tall buildings with soil structure interaction", *Interaction Multiscale Mech.*, **6**(4), 339-356. https://doi.org/10.12989/imm.2013.6.4.339

FEMA P-695 (2009), *Quantification of Building Seismic Performance Factors*, Federal Emergency Management Agency, Washington DC., USA.

Ghaboussi, J. and Joghataie, A. (1995), "Active control of structures using neural networks", *J. Struct. Eng. ASCE*, **115**, 2897-2913. https://doi.org/10.1061/(asce)0733-9399(1995)121:4(555)

Ghaffarzadeh, H. and Younespour, A. (2014), "Active tendons control of structures using block pulse functions", *Struct. Contorl Health Monitor.*, **21**, 1453-1464. https://doi.org/10.1002/stc.1656

Guclu, R. (2006), "Sliding Mode and PID Control of a Structural System against Earthquake", *Math. Comput. Modelling*, **44**, 210-217.

Guclu R. and Yazıcı H. (2008), "Vibration control of a structure with ATMD against earthquake using fuzzy Logic controllers", *J. Sound Vib.,* **318**, 36-49. https://doi.org/10.1016/j.jsv.2008.03.058.

Liu, M.Y., Chiang, W.L., Hwang, J.H. and Chu, C.R. (2008), "Wind-induced vibration of high-rise building with tuned mass damper including soil- structure interaction", *J. Wind Eng. Industrial Aerodynam.*, https://doi.org/10.1016/j.jweia.2007.06.034.

Makris, N. (1997), "Rigidity-Plasticity-Viscosity: Can electrorheological dampers protect base-isolated structures from near-source ground motions?", *Earthq. Eng. Struct. Dynam*., **26**, 571-591. https://doi.org/10.1002/(sici)1096-9845(199705)26:5<571::aid-eqe658>3.0.co;2-6.

MathWorks Inc. (2015), MATLAB R2015b.Natick, MA, USA.

Nazarimofrad, E. and Zahrai, S.M., (2016), "Seismic control of irregular multistory buildings using active tendons considering soil-structure interaction effect", *Soil Dynam. Earthq. Eng.* **89**, 100-115. https://doi.org/10.1016/j.soildyn.2016.07.005.

Nerves, A.C. and Krishnan, R. (1995), Active control strategies for tall civil structures, *Motion Control Systems Research Group*, VA 24061-0111. https://doi.org/10.1109/iecon.1995.483859.

Nigdeli, S.M. and Boduroglu, B.H., (2013), "Active Tendon Control of Torsionally Irregular Structures under Near-Fault Ground Motion Excitation", *Computer-Aided Civil Infrasstructure Eng.*, **28**, 718-736. https://doi.org/10.1111/mice.12046.

Rao, R.V., Savsani, V.J. and Vakharia, D.P. (2011), "Teaching-learning-based optimization: a novel method for constrained mechanical design optimization problems", *Comput. Aided Design*, **43**(3), 303-315. https://doi.org/10.1016/j.cad.2010.12.015.

Rao, R.V (2016), "Jaya: A simple and new optimization algorithm for solving constrained and unconstrained optimization problems", *J. Industrial Eng. Comput.*, **7**(1), 19-34. https://doi.org/10.5267/j.ijiec.2015.8.004.

Samali, B., Yang, J.N. and Liu, S.C, (1985), "Active control of seismic-excited buildings", *J. Struct. Eng. ASCE*, **111**, 2165-2180. https://doi.org/10.1061/(asce)0733-9445(1985)11110(2165).

Sommerville, P.G. (2003), "Magnitude scaling of the near fault rupture directivity pulse", *Phys. Earth Planetary Interiors*, **137**,201–212. https://doi.org/10.1016/s0031-9201(03)00015-3.

Toklu, Y.C. and Arditi, D. (2014), "Smart trusses for space applications", *14th ASCE International Conference on Engineering, Science, Construction and Operations in Challenging Environments, Earth and Space, Engineering for Extreme Environment*, St. Louis, Missouri, USA, October.

Yakut, O. and Alli, H., (2011), "Neural based sliding-mode control with moving sliding surface for the seismic isolation of structures", *J. Vib. Control*, **17**, 2103-2116. https://doi.org/10.1177/1077546310395964.

Yang, J.N. and Samali, B. (1983), "Control of tall buildings in along-wind motion", *J. Struct. Eng. ASCE*, **109**, 50-68. https://doi.org/10.1061/(asce)0733-9445(1983)109:1(50).

Yang, X.S. (2010), *Engineering Optimization: An Introduction with Metaheuristic Applications*, John Wiley and Sons, New Jersey, USA. https://doi.org/10.1002/9780470640425.

Yang, X.S., Karamanoglu, M. and He, X. (2014), "Flower pollination algorithm: A novel approach for multiobjective optimization", *Eng. Optimization*, **46**(9), 1222-1237. https://doi.org/10.1080/0305215x.2013.832237.

Zou, L., Fang, L., Huang, K. and Wang, L. (2012), "Vibration control of soil-structure systems and Pile-Soil-Structure systems", *KSCE J. Civil Eng.*, **16**(5), 794-802. https://doi.org/10.1007/s12205-012-1358-2.

CC

Appendix

Table 6 The maximum responses of structure under near fault ground motions without pulse according to FPA (dense soil)

EQ	CPNT	Displacement (cm)				Acceleration (m/s^2)				Control signal (cm)	Control force (KN)
		Uncontrolled		Controlled		Uncontrolled		Controlled		Controlled	Controlled
		1.floor	15.floor	1.floor	15.floor	1.floor	15.floor	1.floor	15.floor	each floor	each floor
1	FN	20.42	30.71	19.38	26.57	3.08	3.27	2.75	2.96	5.93	71.40
	FP	46.87	55.64	36.25	44.36	3.43	3.54	3.05	3.36	8.31	100.0
2	FN	24.54	29.96	19.05	22.09	3.11	3.18	2.91	2.96	6.08	73.24
	FP	12.32	14.93	10.16	11.36	1.96	2.01	1.99	1.96	3.36	40.50
3	FN	19.77	26.82	11.10	15.42	1.48	1.79	1.41	1.71	4.47	53.86
	FP	28.42	38.72	16.68	22.70	2.74	3.20	2.44	2.65	5.74	69.14
4	FN	66.42	94.05	47.98	69.01	3.90	4.26	3.72	3.74	7.76	93.40
	FP	21.93	29.68	18.80	25.92	1.31	1.69	1.30	1.46	4.72	56.78
5	FN	34.65	48.32	28.23	40.28	1.71	1.92	1.25	1.56	4.92	59.30
	FP	24.45	33.12	19.89	26.04	1.69	1.85	1.55	1.66	3.00	36.13
6	FN	22.38	29.71	17.19	22.29	2.17	2.22	1.84	1.96	5.10	61.47
	FP	17.64	23.85	18.14	24.59	2.01	2.08	2.05	2.08	3.36	40.51
7	FN	6.770	8.290	6.500	7.860	0.64	0.71	0.63	0.64	1.58	19.02
	FP	8.670	11.87	8.340	12.64	0.82	1.08	0.81	1.06	2.18	26.23
8	FN	74.37	107.1	64.88	91.89	3.06	4.19	2.83	3.50	11.2	134.9
	FP	86.91	118.3	54.73	74.29	2.89	3.72	2.37	2.56	7.91	95.29
9	FN	25.09	34.66	16.66	24.22	1.07	1.24	0.76	0.95	2.87	34.57
	FP	31.30	42.06	22.14	31.10	2.60	3.02	2.38	2.32	4.50	54.17
10	FN	9.230	12.53	6.910	8.910	0.67	0.77	0.60	0.69	1.64	19.76
	FP	8.180	11.42	7.760	10.17	1.06	1.23	1.01	1.16	2.36	28.43
11	FN	19.41	29.06	14.54	18.49	1.41	1.63	1.20	1.33	4.08	49.18
	FP	37.10	50.77	27.83	37.13	2.81	3.09	2.56	2.98	7.07	85.09
12	FN	48.58	71.12	40.37	56.84	2.16	2.85	2.07	2.73	6.22	74.88
	FP	81.36	118.6	44.60	58.05	3.61	4.84	2.84	3.06	5.98	72.04
13	FN	67.06	92.92	51.21	66.38	11.0	12.9	10.7	11.7	19.5	234.7
	FP	55.03	75.80	31.59	48.10	5.31	6.22	4.55	5.11	8.16	98.23
14	FN	164.8	227.1	86.78	120.3	4.87	6.70	3.01	3.70	11.6	139.6
	FP	115.6	159.9	72.70	102.5	3.27	4.56	2.40	2.99	9.83	118.4

EQ: Earthquake, CPNT: Component, FN: Fault normal, FP: Fault parallel

Table 7 The maximum responses of structure under near fault ground motions without pulse according to FPA (medium soil)

EQ	CPNT	Displacement (cm)				Acceleration (m/s^2)				Control signal (cm)	Control force (KN)
		Uncontrolled		Controlled		Uncontrolled		Controlled		Controlled	Controlled
		1.floor	15.floor	1.floor	15.floor	1.floor	15.floor	1.floor	15.floor	each floor	each floor
1	FN	20.42	30.71	19.37	26.55	3.08	3.27	2.79	2.95	5.83	70.20
	FP	46.87	55.64	36.17	44.30	3.43	3.54	3.09	3.38	8.25	99.39
2	FN	24.54	29.96	19.00	22.05	3.11	3.18	2.90	2.92	6.00	72.25
	FP	12.32	14.93	10.14	11.34	1.96	2.01	1.99	1.97	3.33	40.04
3	FN	19.77	26.82	11.09	15.38	1.48	1.79	1.42	1.72	4.42	53.21
	FP	28.42	38.72	16.81	22.53	2.74	3.20	2.43	2.64	5.67	68.32
4	FN	66.42	94.05	47.74	68.89	3.90	4.26	3.71	3.73	7.71	92.89
	FP	21.93	29.68	18.79	25.90	1.31	1.69	1.30	1.46	4.64	55.81
5	FN	34.65	48.32	28.16	40.22	1.71	1.92	1.26	1.57	4.92	59.28
	FP	24.45	33.12	19.87	25.98	1.69	1.85	1.56	1.66	3.02	36.35
6	FN	22.38	29.71	17.12	22.27	2.17	2.22	1.83	1.94	5.06	60.92
	FP	17.64	23.85	18.09	24.58	2.01	2.08	2.02	2.06	3.32	39.95
7	FN	6.770	8.290	6.490	7.85	0.64	0.71	0.63	0.64	1.54	18.52
	FP	8.670	11.87	8.270	12.59	0.82	1.08	0.77	1.02	2.14	25.73
8	FN	74.37	107.1	64.84	91.72	3.06	4.19	2.84	3.50	1.17	134.5
	FP	86.91	118.3	54.62	74.11	2.89	3.72	2.37	2.55	7.86	94.66
9	FN	25.09	34.66	16.65	24.18	1.07	1.24	0.76	0.95	2.86	34.48
	FP	31.30	42.06	22.12	31.03	2.60	3.02	2.37	2.33	4.48	53.91
10	FN	9.230	12.53	6.900	8.900	0.67	0.77	0.60	0.69	1.62	19.51
	FP	8.180	11.42	7.760	10.15	1.06	1.23	1.00	1.16	2.33	28.06
11	FN	19.41	29.06	14.49	18.50	1.41	1.63	1.19	1.32	4.03	48.55
	FP	37.10	50.77	27.64	37.17	2.81	3.09	2.58	3.00	7.00	84.24
12	FN	48.58	71.12	40.19	56.77	2.16	2.85	2.08	2.73	6.18	74.44
	FP	81.36	118.6	44.46	57.66	3.61	4.84	2.85	3.07	5.97	71.88
13	FN	67.06	92.92	51.71	65.80	11.0	12.9	10.7	11.7	19.2	231.1
	FP	55.03	75.80	31.81	48.09	5.31	6.22	4.58	5.14	8.18	98.44
14	FN	164.8	227.1	86.54	120.0	4.87	6.70	3.01	3.71	11.5	139.0
	FP	115.6	159.9	72.64	102.3	3.27	4.56	2.38	2.98	9.85	118.5

EQ: Earthquake, CPNT: Component, FN: Fault normal, FP: Fault parallel

Table 8 The maximum responses of structure under near fault ground motions without pulse according to TLBO (soft soil)

EQ	CPNT	Displacement (cm)				Acceleration (m/s^2)				Control signal (cm)	Control force (KN)
		Uncontrolled		Controlled		Uncontrolled		Controlled		Controlled	Controlled
		1.floor	15.floor	1.floor	15.floor	1.floor	15.floor	1.floor	15.floor	each floor	each floor
1	FN	20.42	30.71	19.01	26.05	3.08	3.27	2.58	2.57	6.36	76.53
	FP	46.87	55.64	33.88	43.07	3.43	3.54	3.06	3.14	8.50	102.3
2	FN	24.54	29.96	18.36	22.10	3.11	3.18	2.65	2.62	6.32	76.15
	FP	12.32	14.93	9.750	11.07	1.96	2.01	1.82	1.83	3.57	42.98
3	FN	19.77	26.82	10.57	14.93	1.48	1.79	1.44	1.73	4.81	57.87
	FP	28.42	38.72	16.39	20.74	2.74	3.20	1.88	2.00	6.00	72.22
4	FN	66.42	94.05	43.32	67.82	3.90	4.26	3.43	3.44	7.72	92.90
	FP	21.93	29.68	18.28	25.41	1.31	1.69	1.29	1.48	4.93	59.42
5	FN	34.65	48.32	27.35	39.49	1.71	1.92	1.31	1.65	5.14	61.86
	FP	24.45	33.12	20.09	25.94	1.69	1.85	1.63	1.69	3.18	38.32
6	FN	22.38	29.71	16.12	21.85	2.17	2.22	1.65	1.79	5.27	63.49
	FP	17.64	23.85	17.35	24.60	2.01	2.08	1.66	1.77	3.53	42.53
7	FN	6.770	8.290	5.760	7.740	0.64	0.71	0.55	0.66	1.59	19.16
	FP	8.670	11.87	8.080	12.19	0.82	1.08	0.69	0.84	2.34	28.21
8	FN	74.37	107.1	64.47	89.75	3.06	4.19	2.87	3.39	11.1	133.3
	FP	86.91	118.3	54.07	73.39	2.89	3.72	2.27	2.48	7.77	93.50
9	FN	25.09	34.66	16.11	23.39	1.07	1.24	0.76	0.91	2.92	35.19
	FP	31.30	42.06	21.63	29.98	2.60	3.02	2.04	2.24	4.52	54.38
10	FN	9.230	12.53	6.710	8.700	0.67	0.77	0.58	0.67	1.77	21.34
	FP	8.180	11.42	7.630	9.68	1.06	1.23	0.92	1.08	2.53	30.49
11	FN	19.41	29.06	14.11	18.93	1.41	1.63	1.23	1.32	4.05	48.81
	FP	37.10	50.77	25.85	37.68	2.81	3.09	2.60	3.02	7.17	83.22
12	FN	48.58	71.12	39.20	57.60	2.16	2.85	2.00	2.69	6.07	73.14
	FP	81.36	118.6	43.00	57.00	3.61	4.84	2.71	3.26	6.33	76.21
13	FN	67.06	92.92	48.66	61.11	11.0	12.9	8.21	9.02	18.1	218.3
	FP	55.03	75.80	32.05	41.53	5.31	6.22	3.82	3.69	6.82	82.14
14	FN	164.8	227.1	86.53	120.8	4.87	6.70	3.12	3.95	11.81	142.2
	FP	115.6	159.9	71.75	100.3	3.27	4.56	2.43	3.01	9.83	118.4

EQ: Earthquake, CPNT: Component, FN: Fault normal, FP: Fault parallel

Table 9 The maximum responses of structure under near fault ground motions with pulse according to FPA (dense soil)

EQ	CPNT	Displacement (cm)				Acceleration (m/s^2)				Control signal (cm)	Control force (KN)
		Uncontrolled		Controlled		Uncontrolled		Controlled		Controlled	Controlled
		1.floor	15.floor	1.floor	15.floor	1.floor	15.floor	1.floor	15.floor	each floor	each floor
1	FN	27.21	35.25	20.85	26.84	1.43	1.50	1.26	1.24	3.38	40.75
	FP	72.22	100.1	53.17	72.23	2.32	3.36	2.11	2.56	7.10	85.45
2	FN	61.69	80.48	57.71	75.28	3.70	3.97	3.05	3.87	9.36	112.7
	FP	58.07	80.85	33.21	45.40	2.07	2.59	1.75	2.26	4.92	59.24
3	FN	53.13	77.63	38.75	56.94	2.65	3.02	2.07	2.44	6.54	78.71
	FP	87.60	115.7	60.84	87.67	4.06	4.72	3.49	3.91	8.66	104.3
4	FN	59.81	80.83	42.61	57.56	2.21	3.11	2.07	2.62	5.76	69.40
	FP	45.57	63.36	39.35	55.06	2.26	2.73	1.96	2.64	8.14	98.07
5	FN	65.58	91.72	51.90	69.80	3.16	3.79	2.40	2.89	7.37	88.76
	FP	149.7	207.3	110.3	153.8	4.98	6.55	3.38	5.11	14.1	170.1
6	FN	49.20	67.63	30.90	39.63	2.05	2.62	1.53	1.91	4.25	51.12
	FP	131.0	181.1	85.00	114.4	4.41	5.78	3.36	4.65	11.7	140.9
7	FN	38.27	52.84	24.24	35.54	2.05	2.32	1.39	1.58	3.45	41.58
	FP	36.48	51.00	17.48	25.76	1.20	1.62	0.87	1.17	2.58	31.10
8	FN	130.3	180.5	86.67	121.5	3.72	5.12	2.83	3.86	10.4	125.0
	FP	38.52	53.43	26.28	38.60	1.49	1.92	1.11	1.57	4.20	50.53
9	FN	21.46	31.96	16.80	23.93	1.95	2.26	1.85	2.01	4.38	52.71
	FP	46.15	60.07	38.15	46.59	3.83	3.80	3.55	3.68	7.29	87.78
10	FN	62.22	78.44	43.76	63.57	4.97	5.26	4.67	4.80	10.7	128.2
	FP	33.07	47.16	26.84	44.18	2.24	2.76	2.08	2.70	7.00	84.26
11	FN	27.36	38.09	19.53	27.68	1.11	1.51	0.93	1.43	3.85	43.34
	FP	45.95	64.03	37.97	52.64	2.21	2.67	2.05	2.24	5.26	63.35
12	FN	48.78	66.16	33.12	47.59	3.22	3.57	2.70	2.91	8.00	96.38
	FP	52.72	75.56	42.51	60.08	2.88	3.59	2.48	3.42	8.43	101.5
13	FN	234.4	322.7	117.2	166.5	7.91	10.2	4.59	5.56	16.1	194.1
	FP	75.80	105.1	53.19	71.74	2.68	3.74	2.31	2.49	9.30	112.0
14	FN	95.77	131.9	70.98	97.92	3.08	4.01	2.32	2.89	9.29	111.9
	FP	84.85	118.4	52.67	73.18	3.07	4.08	2.38	2.90	9.17	110.4

EQ: Earthquake, CPNT: Component, FN: Fault normal, FP: Fault parallel

Table 10 The maximum responses of structure under near fault ground motions with pulse according to FPA (medium soil)

EQ	CPNT	Displacement (cm)				Acceleration (m/s^2)				Control signal (cm)	Control force (KN)
		Uncontrolled		Controlled		Uncontrolled		Controlled		Controlled	Controlled
		1.floor	15.floor	1.floor	15.floor	1.floor	15.floor	1.floor	15.floor	each floor	each floor
1	FN	27.21	35.25	20.82	26.84	1.43	1.50	1.25	1.23	3.37	40.61
	FP	72.22	100.1	53.15	72.14	2.32	3.36	2.12	2.58	7.10	85.45
2	FN	61.69	80.48	57.56	75.38	3.70	3.97	3.00	3.91	9.32	112.3
	FP	58.07	80.85	33.19	45.15	2.07	2.59	1.76	2.28	4.91	59.11
3	FN	53.13	77.63	38.62	56.71	2.65	3.02	2.08	2.45	6.46	77.74
	FP	87.60	115.7	60.71	87.34	4.06	4.72	3.50	3.92	8.65	104.1
4	FN	59.81	80.83	45.52	56.56	2.21	3.11	2.09	2.65	5.73	69.52
	FP	45.57	63.36	39.26	55.06	2.26	2.73	1.97	2.65	8.07	97.19
5	FN	65.58	91.72	51.86	69.69	3.16	3.79	2.39	2.88	7.35	88.45
	FP	149.7	207.3	110.1	153.6	4.98	6.55	3.40	5.14	14.2	170.7
6	FN	49.20	67.63	30.84	39.52	2.05	2.62	1.53	1.92	4.24	51.03
	FP	131.0	181.1	84.79	114.4	4.41	5.78	3.35	4.64	11.6	140.1
7	FN	38.27	52.84	24.18	35.59	2.05	2.32	1.40	1.59	3.46	41.68
	FP	36.48	51.00	17.41	25.72	1.20	1.62	0.87	1.18	2.58	31.01
8	FN	130.3	180.5	86.42	121.2	3.72	5.12	2.82	3.86	10.4	125.3
	FP	38.52	53.43	26.24	38.56	1.49	1.92	1.11	1.57	4.20	50.55
9	FN	21.46	31.96	16.79	23.89	1.95	2.26	1.85	1.99	4.31	51.94
	FP	46.15	60.07	38.16	46.44	3.83	3.80	3.57	3.69	7.22	86.90
10	FN	62.22	78.44	43.71	63.51	4.97	5.26	4.67	4.81	10.5	127.2
	FP	33.07	47.16	26.81	44.18	2.24	2.76	2.10	2.70	6.97	83.95
11	FN	27.36	38.09	19.48	27.68	1.11	1.51	0.95	1.44	3.814	45.84
	FP	45.95	64.03	37.91	52.51	2.21	2.67	2.06	2.25	5.25	63.48
12	FN	48.78	66.16	33.13	47.53	3.22	3.57	2.69	2.89	7.97	96.00
	FP	52.72	75.56	42.50	60.09	2.88	3.59	2.50	3.43	8.40	101.2
13	FN	234.4	322.7	116.8	165.8	7.91	10.2	4.57	5.51	16.09	193.7
	FP	75.80	105.1	53.17	71.44	2.68	3.74	2.33	2.50	9.24	111.2
14	FN	95.77	131.9	70.85	97.79	3.08	4.01	2.31	2.90	9.25	111.1
	FP	84.85	118.4	52.67	72.82	3.07	4.08	2.38	2.89	9.00	109.1

EQ: Earthquake, CPNT: Component, FN: Fault normal, FP: Fault parallel

Table 11 The maximum responses of structure under near fault ground motions with pulse according to TLBO (soft soil)

EQ	CPNT	Displacement (cm)				Acceleration (m/s^2)				Control signal (cm)	Control force (KN)
		Uncontrolled		Controlled		Uncontrolled		Controlled		Controlled	Controlled
		1.floor	15.floor	1.floor	15.floor	1.floor	15.floor	1.floor	15.floor	each floor	each floor
1	FN	27.21	35.25	20.20	26.17	1.43	1.50	1.15	1.18	3.59	43.28
	FP	72.22	100.1	52.20	70.46	2.32	3.36	2.13	2.61	6.71	80.74
2	FN	61.69	80.48	53.97	74.53	3.70	3.97	2.94	4.02	10.4	125.0
	FP	58.07	80.85	33.94	45.87	2.07	2.59	1.70	2.09	4.74	57.10
3	FN	53.13	77.63	39.08	56.51	2.65	3.02	2.15	2.61	6.45	77.72
	FP	87.60	115.7	61.03	86.18	4.06	4.72	3.30	3.80	9.02	108.6
4	FN	59.81	80.83	40.53	56.97	2.21	3.11	2.15	2.77	5.82	70.10
	FP	45.57	63.36	37.18	53.40	2.26	2.73	1.85	2.72	8.44	101.7
5	FN	65.58	91.72	50.81	67.97	3.16	3.79	2.17	2.66	7.22	86.93
	FP	149.7	207.3	107.5	151.2	4.98	6.55	3.34	5.27	14.4	173.2
6	FN	49.20	67.63	29.82	39.35	2.05	2.62	1.49	1.96	4.24	51.02
	FP	131.0	181.1	81.85	113.0	4.41	5.78	3.10	4.34	11.6	139.0
7	FN	38.27	52.84	23.64	34.65	2.05	2.32	1.42	1.66	3.49	42.08
	FP	36.48	51.00	16.97	25.52	1.20	1.62	0.96	1.27	2.72	32.81
8	FN	130.3	180.5	86.40	121.1	3.72	5.12	2.79	3.88	10.7	128.6
	FP	38.52	53.43	25.78	38.01	1.49	1.92	1.18	1.63	4.50	54.20
9	FN	21.46	31.96	16.71	22.00	1.95	2.26	1.65	1.77	4.56	54.92
	FP	46.15	60.07	37.38	44.51	3.83	3.80	3.58	3.61	7.66	92.27
10	FN	62.22	78.44	42.79	62.16	4.97	5.26	4.43	4.82	11.3	136.0
	FP	33.07	47.16	25.76	41.54	2.24	2.76	1.82	2.55	7.52	90.57
11	FN	27.36	38.09	18.78	27.53	1.11	1.51	1.12	1.52	4.08	49.10
	FP	45.95	64.03	37.74	51.93	2.21	2.67	2.05	2.29	5.21	62.75
12	FN	48.78	66.16	31.78	45.01	3.22	3.57	2.20	2.68	8.37	100.8
	FP	52.72	75.56	41.61	57.69	2.88	3.59	2.65	3.49	8.82	106.3
13	FN	234.4	322.7	120.5	169.4	7.91	10.2	4.31	5.30	16.1	193.6
	FP	75.80	105.1	53.80	69.61	2.68	3.74	2.72	2.99	9.35	112.6
14	FN	95.77	131.9	69.79	97.00	3.08	4.01	2.15	3.02	9.28	111.7
	FP	84.85	118.4	54.01	72.44	3.07	4.08	2.11	2.51	8.44	101.6

EQ: Earthquake, CPNT: Component, FN: Fault normal, FP: Fault parallel